

# Optical sensing by optimized silicon slot waveguides

Francesco Dell'Olio and Vittorio M. N. Passaro

Dipartimento di Elettrotecnica ed Elettronica, Politecnico di Bari, Via E. Orabona 4, 70125 Bari, Italy  
E-mail: [passaro@deemail.poliba.it](mailto:passaro@deemail.poliba.it), WEB page: <http://dee.poliba.it/photonicsgroup>

**Abstract:** A theoretical investigation of silicon-on-insulator nanometer slot waveguides for highly sensitive and compact chemical and biochemical integrated optical sensing is proposed. Slot guiding structures enabling high optical confinement in a low-index very small region are demonstrated to be very sensitive to either cover medium refractive index change or deposited receptor layer thickness increase. Modal and confinement properties of slot waveguides have been investigated, considering also the influence of fabrication tolerances. Waveguide sensitivity has been calculated and compared with that exhibited by other silicon nanometer guiding structures, such as rib or wire waveguides, or with experimental values in literature.

©2007 Optical Society of America

**OCIS codes:** (040.6040) Silicon; (130.0130) Integrated optics; (130.3120) Integrated Optics Devices; (130.6010) Sensors.

---

## References and links

1. S. Balslev, A. M. Jorgensen, B. Bilenberg, K. B. Mogensen, D. Snakenborg, O. Geschke, J. P. Kutter, and A. Kristensen, "Lab-on-a-chip with integrated optical transducers," *Lab on a Chip* **6**, 213 (2006).
2. B. J. Luff, R. D. Harris, J. S. Wilkinson, R. Wilson, and D. J. Schiffrin, "Integrated-optical directional coupler biosensor," *Opt. Lett.* **21**, 618 (1996).
3. F. Prieto, B. Sepulveda, A. Calle, A. Llobera, C. Domynguez, A. Abad, A. Montoya, and L M Lechuga, "An integrated optical interferometric nanodevice based on silicon technology for biosensor applications," *Nanotechnology* **14**, 907 (2003).
4. W. C. L. Hopman, P. Pottier, D. Yudistira, J. van Lith, P. V. Lambeck, R. M. De La Rue, and A. Driessen, "Quasi-One-Dimensional Photonic Crystal as a Compact Building-Block for Refractometric Optical Sensors," *IEEE J. Sel. Top. Quantum Electron.* **11**, 11 (2005).
5. C. Y. Chao, W. Fung, and L. J. Guo, "Polymer Microring Resonators for Biochemical Sensing Applications," *IEEE J. Sel. Top. Quantum Electron.* **12**, 134 (2006).
6. B. Jalali and S. Fathpour, "Silicon Photonics," *J. Lightwave Technol.* **24**, 4600 (2006).
7. H. Yamada, T. Chu, S. Ispida, and Y. Arakawa, "Si Photonic Wire Waveguide Devices," *IEEE J. Sel. Top. Quantum Electron.* **12**, 1371 (2006).
8. A. Densmore, D.-X. Xu, P. Waldron, S. Janz, P. Cheben, J. Lapointe, A. Del age, B. Lamontagne, J. H. Schmid, and E. Post, "A Silicon-on-Insulator Photonic Wire Based Evanescent Field Sensor," *IEEE Photon. Technol. Lett.* **18**, 2520 (2006).
9. F. Dell'Olio, V. M. N. Passaro, and F. De Leonardi, "Ammonia Optical Sensing by Microring Resonators," in *Proc. of 11<sup>th</sup> Int. Meeting on Chemical Sensors*, G. Sberveglieri, ed. (Publisher, Brescia, 2006), p. 27.
10. Q. Xu, V. R. Almeida, R. R. Panepucci, and M. Lipson, "Experimental demonstration of guiding and confining light in nanometer-size low-refractive-index material," *Opt. Lett.* **29**, 1626 (2004).
11. T. Baehr-Jones, M. Hochberg, G. Wang, R. Lawson, Y. Liao, P. A. Sullivan, L. Dalton, A. K.-Y. Jen, and A. Scherer, "Optical modulation and detection in slotted silicon waveguides," *Opt. Express* **13**, 5216 (2005).
12. C. A. Barrios and M. Lipson, "Electrically driven silicon resonant light emitting device based on slot-waveguide," *Opt. Express* **13**, 10092 (2005).
13. T. Fujisawa and M. Koshiba, "Polarization-independent optical directional coupler based on slot waveguides," *Opt. Lett.* **31**, 56 (2006).
14. T. Fujisawa and M. Koshiba, "All-optical logic gates based on nonlinear slot-waveguide couplers," *J. Opt. Soc. Am. B* **23**, 684 (2006).
15. T. Fujisawa and M. Koshiba, "Theoretical Investigation of Ultrasmall Polarization-Insensitive 1x2 Multimode Interference Waveguides Based on Sandwiched Structures," *IEEE Photon. Technol. Lett.* **18**, 1246 (2006).
16. P. M ullner and R. Hainberger, "Structural Optimization of Silicon-On-Insulator Slot Waveguides," *IEEE Photon. Technol. Lett.* **18**, 2557 (2006).

17. R. Bernini, N. Cennamo, A. Minardo, and L. Zeni, "Planar Waveguides for Fluorescence-Based Biosensing: Optimization and Analysis," *IEEE Sens. J.* **6**, 1218 (2006).
  18. R. Bernini, N. Cennamo, A. Minardo, and L. Zeni, "Silicon planar waveguides for absorption based biosensors," *Proc. of 1<sup>st</sup> Int. Workshop on Advances in sensors and interfaces*, D. De Venuto and B. Courtois, ed. (Laterza, Bari, 2005), pp. 138-142.
  19. Comsol Multiphysics by COMSOL ©, ver. 3.2, single license (2005).
  20. O. Parriaux and G. J. Valdhuis, "Normalized Analysis for the Sensitivity Optimization of Integrated Optical Evanescent-Wave Sensors," *J. Lightwave Technol.* **16**, 573 (1998).
  21. O. Parriaux, G. J. Valdhuis, H. J. W. M. Hoekstra, and P. V. Lambeck "Sensitivity Enhancement in Evanescent Optical Waveguide Sensors," *J. Lightwave Technol.* **18**, 677 (2000).
  22. F. Dell'Olio, V. M. N. Passaro, and F. De Leonardis, "Surface Sensitivity Optimization of a Microring Resonator for Biochemical Sensing," in *Proc. of 8<sup>th</sup> Int. Conf. on Transparent Optical Networks*, M. Marciniak, Ed. (National Institute of Telecommunications, 2006) **4**, pp. 128-131.
- 

## 1. Introduction

Optical technologies play a central role in chemical and biochemical analysis and their employment in *lab-on-a-chip* micro-systems has been demonstrated as very attractive [1]. In this framework, optical chemical sensing by guided-wave devices has been reaching a considerable attention. Different integrated optical chemical and biochemical sensors have been proposed, such as those based on directional couplers [2], Mach-Zehnder interferometers [3], Bragg gratings [4], and microring resonators [5]. In these sensors the concentration change of a chemical analyte to be sensed affects the propagating mode effective index, which is measured in different ways, according with sensor architecture. The effective index change is produced either by a change of cover medium refractive index (*homogeneous sensing*) or by a change of thickness of an ultra-thin layer of receptor molecules which are immobilized on waveguide surface (*surface sensing*). Measurement sensitivity depends on optical field distribution in the cover medium, so one of the most important design task is the waveguide optimization in order to maximize its sensitivity.

Silicon technology in high performance photonic devices and optical integrated circuits has been demonstrated as a very interesting prospective for a great number of application fields, including sensors. For example, silicon integrated lab-on-a-chip systems in which photonic sensing functions are integrated with electronic intelligence and wireless communications can be employed in environmental monitoring and medical diagnostics [6].

Recently, Silicon-on-Insulator (SOI) sub-micrometer silicon wire waveguides [7] have been demonstrated very attractive for integrated optical sensors, because they exhibit a sensitivity significantly larger than that assured by other guiding structures based on silicon oxynitride (SiON), polymeric materials or silica [8]. Using a Si-wire waveguide, a highly sensitive microring resonator-based ammonia optical sensor has been proposed [9].

When two Si-wires are very close to each other, it is possible to realize another SOI nanometer guiding structure, usually known as SOI slot waveguide [10]. A great variety of optical devices has been recently proposed or fabricated by using slot waveguides, including microring resonators [10], optical modulators [11], electrically pumped light emitting devices [12], directional couplers [13], all-optical logic gates [14] and beam splitters [15]. Moreover, a Finite Element Method (FEM)-based modal investigation devoted to study the influence of slot waveguide geometrical parameters on optical power fraction confined in the low-index gap region has been also carried out [16].

However, SOI slot waveguides for integrated optical sensors represents a quite unexplored research field. Planar slot waveguides for fluorescence- or absorption-based optical biosensing have been only proposed [17-18].

In this paper, we perform a detailed SOI slot waveguide modal investigation, taking into account the fabrication tolerance effect and the possibility that a thin silicon planar layer is placed below the slot structure (in this case, the guiding structure is constituted by two deeply etched nanometer SOI rib waveguides very close to each other, and so it is indicated as *slot rib waveguide*). Sensitivity of both "conventional" slot (without silicon planar layer) and slot

rib waveguides has been investigated and optimized. Calculated sensitivity has been compared with that exhibited by other guiding structures, i.e. SOI rib and Si-wire. Operating wavelength has been always fixed as 1550 nm.

## 2. Modal investigation

### 2.1 Conventional SOI slot waveguides

Conventional SOI slot waveguide (whose structure is shown in Fig. 1(a)) modal behavior has been investigated by full-vectorial 2D FEM [19], assuming as cover medium air, silicon oxide or an aqueous solution (cover medium refractive index  $n_c$  equal to 1, 1.444 or 1.33, respectively).

In FEM mesh generation for effective index and modal profile calculation, triangular vector-elements have been adopted (for example, as in [16]) and maximum element size has been fixed as equal to 2.5 nm in the gap region, 3 nm in the Si wires region, 10 nm in the portion of calculation domain outside both gap region and Si wires region and included in a large rectangle 1  $\mu\text{m}$  wide and 0.45  $\mu\text{m}$  high centred in the centre of the gap region, and 100 nm in the remaining domain portion having a total area of 8  $\mu\text{m}^2$  (4 $\mu\text{m}$ ×2  $\mu\text{m}$ ). In total, we have always used about 100,000 mesh elements. Changing the boundary condition from a perfect electric conductor to a perfect magnetic conductor has a negligible influence on the simulation results. Adopting these mesh parameters, the conventional slot waveguide fabricated in [10] has been simulated. Calculated effective indices (1.757767 for quasi-TM mode and 1.611924 for quasi-TE at the operating wavelength of 1545 nm) are very similar with those experimentally obtained in [10] (relative change lower than 1 %).

Slot guiding structure supports a quasi-TE mode highly confined in the gap region (Fig. 1(b)) and a quasi-TM mode too (Fig. 1(c)). Moreover, slot waveguide fabrication implies silicon deep etching that could produce non vertical side-walls in the structure (see Fig. 1(d)). Waveguide modal profiles, either for quasi-TE or quasi-TM modes, are significantly influenced by this kind of fabrication tolerance (see Fig. 1(d) and Fig. 1(e)). Thus, non vertical sidewall effect on conventional SOI slot waveguide modal properties has been investigated.

Assuming silicon wires with height  $h=250$  nm, width  $w=180$  nm and gap region width  $g=100$  nm, the effective index change as induced by non vertical sidewalls with respect to ideal case (vertical sidewalls), has been calculated. Tilting angle  $\theta$  (see Fig. 1 (d)) with respect to the vertical direction has been varied in the range from 3° to 9°, and quasi-TE and quasi-TM modes have been considered (see Fig. 2). A linear dependence of effective index change on  $\theta$  has been observed for both polarizations. Non vertical sidewalls influence on effective index is stronger for quasi-TE than for quasi-TM mode, because the relevant electric field squared module has its maxima along the vertical interfaces between silicon wires and gap region for quasi-TE mode, while the maxima are outside the gap region for quasi-TM mode. An increase of cover medium refractive index produces a decrease of  $\theta$  influence on effective index, as it is shown in Fig. 2.

Assuming  $\theta=8^\circ$ ,  $g=100$  nm and  $h=250$  nm, the effective index change induced by non vertical sidewalls has been investigated as a function of  $w$  for quasi-TE and quasi-TM modes (Fig. 3). If the cover medium is silicon oxide or an aqueous solution, this change monotonically decreases by increasing the silicon wire width. When cover medium is air, the dependence of effective index shift on  $w$  exhibits a maximum for  $w=180$  nm (maximum values are 20.5 % and 6.15% for quasi-TE and quasi-TM mode, respectively).

The confinement factors in the cover medium  $\Gamma_C$  and in the gap region  $\Gamma_G$  for quasi-TE and quasi-TM modes propagating in slot waveguide can be defined as:

$$\Gamma_C = \frac{\iint |\mathbf{E}(x, y)|^2 dx dy}{\iint_{-\infty}^{\infty} |\mathbf{E}(x, y)|^2 dx dy} \quad \Gamma_G = \frac{\iint |\mathbf{E}(x, y)|^2 dx dy}{\iint_{-\infty}^{\infty} |\mathbf{E}(x, y)|^2 dx dy} \quad (1)$$

where  $\mathbf{E}(x,y)$  is the electric field vector and  $C$  and  $G$  indicate cover medium and gap region, respectively (where gap region is a part of cover medium region, as shown in Fig. 1 (a)).

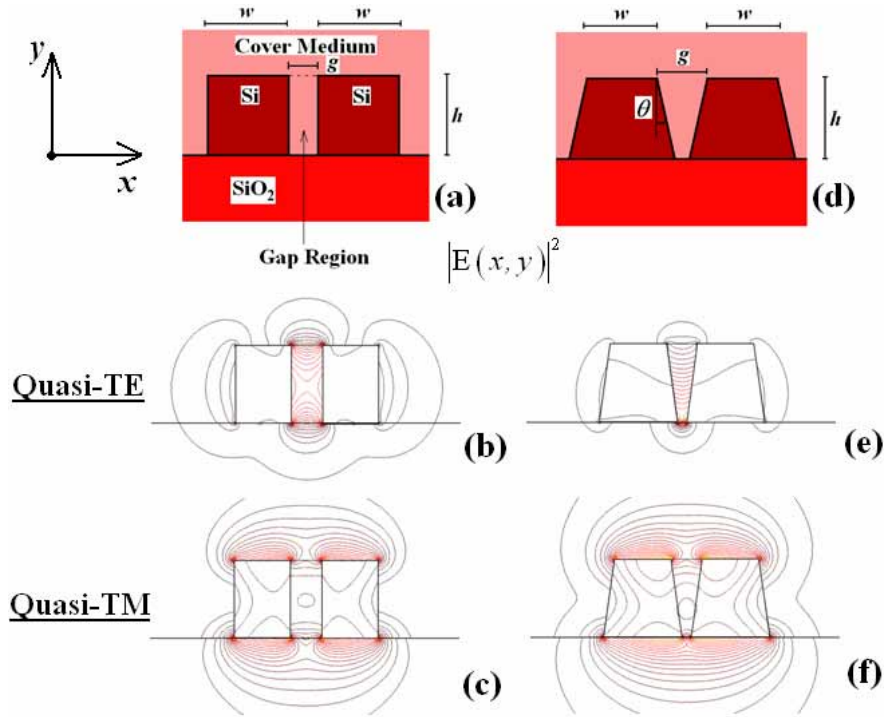


Fig. 1. (a) Conventional SOI slot waveguide structure with vertical sidewalls ( $\theta=0^\circ$ ). (b-c) Relevant electric field squared module for quasi-TE and quasi-TM optical modes. (d) SOI slot waveguide with non vertical sidewalls ( $\theta=8^\circ$ ). (e-f) Relevant electric field squared module for quasi-TE and quasi-TM optical modes. In modal profile calculation, an aqueous solution ( $n_c=1.33$ ) has been assumed as cover medium ( $h=250$  nm,  $w=180$  nm,  $g=100$  nm).

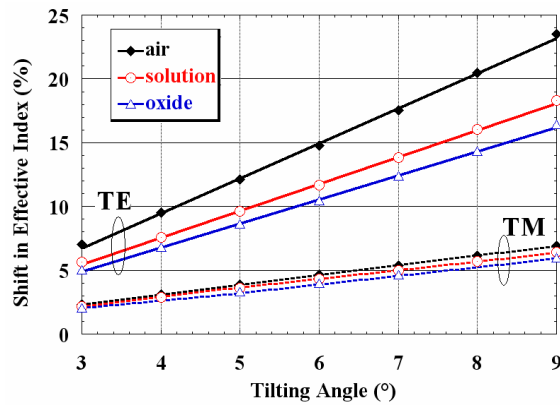


Fig. 2. Percentage shift of quasi-TE and quasi-TM mode effective indices (with respect to vertical case) versus  $\theta$  ( $h=250$  nm,  $w=180$  nm,  $g=100$  nm, conventional slot waveguide), for various cover materials.

Dependence of confinement factors  $\Gamma_C$  and  $\Gamma_G$  on  $w$  has been investigated for  $g=100$  nm and  $h=250$  nm. Effect of non vertical sidewalls ( $\theta=8^\circ$ ) on these factors has been also considered, as shown in Fig. 4. The confinement factors are larger for quasi-TE than for

quasi-TM mode. For quasi-TE mode, non vertical sidewalls produce a decrease in  $\Gamma_C$  and an increase in  $\Gamma_G$ . For quasi-TM mode, non vertical sidewalls produce a decrease of both confinement factors.

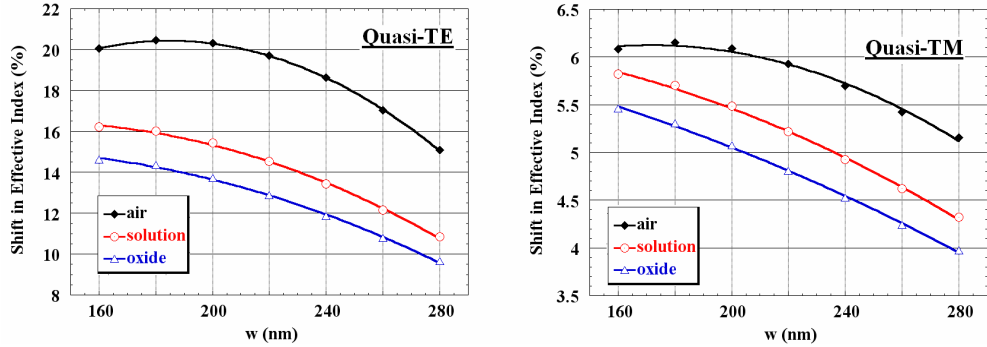


Fig. 3. Percentage shift of quasi-TE and quasi-TM mode effective indices (with respect to vertical case) versus  $w$ , as induced by non vertical sidewalls in conventional slot waveguides ( $h = 250$  nm,  $g = 100$  nm,  $\theta = 8^\circ$ ).

For both polarizations, when the cover medium is an aqueous solution or silicon oxide,  $\Gamma_C$  monotonically decreases when  $w$  increases whereas, when the cover medium is air,  $\Gamma_C$  exhibits a maximum. Confinement factor  $\Gamma_G$  has a maximum in quite all considered cases (only when we consider silicon oxide, non vertical sidewalls and quasi-TM mode,  $\Gamma_G$  dependence on  $w$  is monotone).

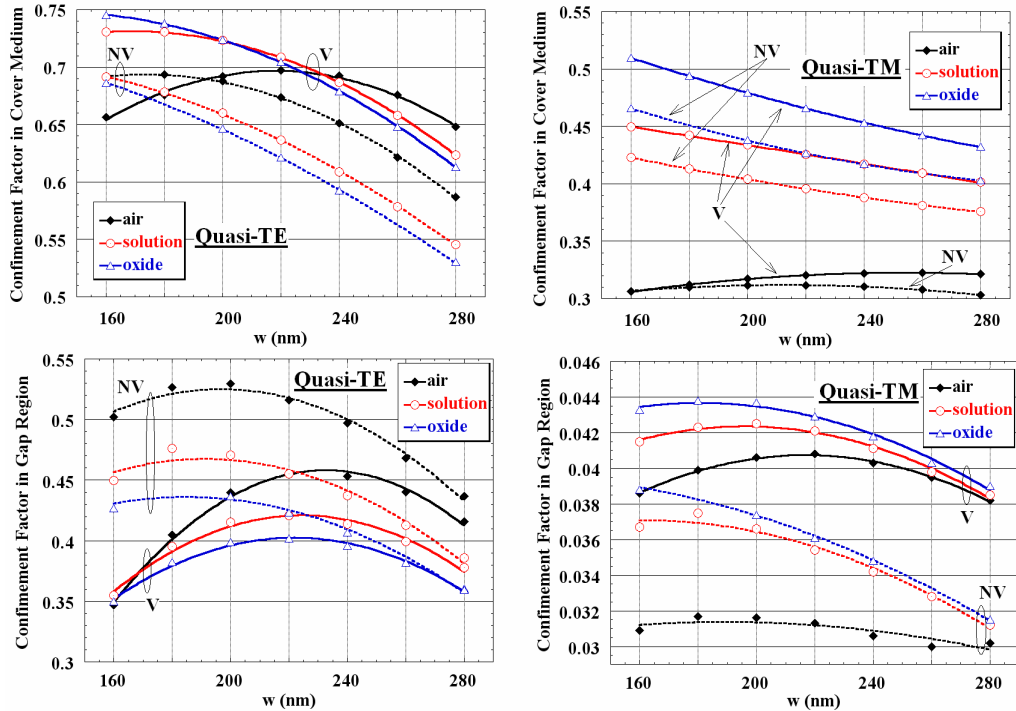


Fig. 4. Conventional SOI slot waveguide confinement factors in cover medium and gap region versus  $w$ , assuming either vertical or non vertical ( $\theta = 8^\circ$ ) sidewalls ( $h = 250$  nm,  $g = 100$  nm).

## 2.2 SOI slot rib waveguides

Optical confinement in low-index medium by total internal reflection can be achieved also maintaining a thin silicon planar layer below the slot structure. The resulting slot rib waveguide is shown in Fig. 5(a). Obviously, non vertical sidewalls (Fig. 5(d)) affect also in this case the waveguide modal distribution either for quasi-TE or quasi-TM modes, as sketched in Fig. 5(b-c) and 5(e-f).

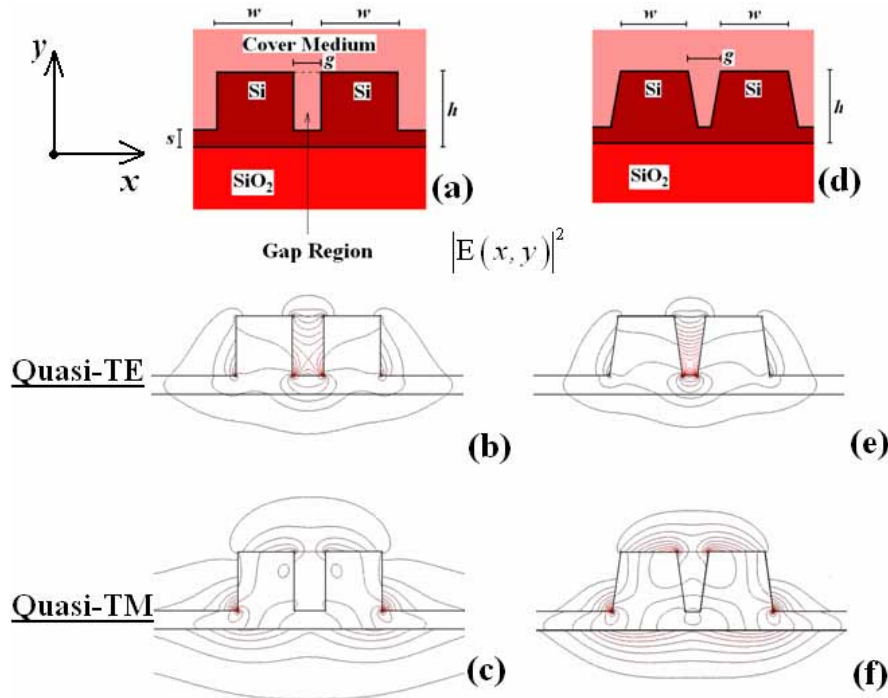


Fig. 5. (a) SOI slot rib waveguide ( $\theta = 0^\circ$ ). (b-c) Quasi-TE and quasi-TM optical modes propagating in the waveguide (squared module of electric field). (d) SOI slot rib waveguide with non vertical sidewalls ( $\theta = 8^\circ$ ). (e-f) Resultant electric field squared module for quasi-TE and quasi-TM optical modes. In modal profile calculation, an aqueous solution has been assumed as cover medium ( $h=250$  nm,  $w=180$  nm,  $g=100$  nm,  $s=60$  nm).

Assuming a waveguide total height  $h=250$  nm, a silicon rib width  $w=180$  nm, a gap region width  $g=100$  nm and a silicon planar layer thickness  $s=60$  nm, non vertical sidewalls tilting angle  $\theta$  influence on effective index has been investigated for quasi-TE and quasi-TM modes (Fig. 6). In mesh generation for FEM calculations, the total number of elements was around 110,000. Comparing Fig. 2 with Fig. 6, it is evident that the presence of a silicon planar layer in the slot structure produces a significant reduction of non vertical sidewalls influence on optical mode effective indices. As in case of conventional slot waveguide, the effective index change linearly depends on  $\theta$ , and non vertical sidewalls influence is stronger for quasi-TE than quasi-TM mode.

Silicon planar layer effect on confinement factors  $\Gamma_C$  and  $\Gamma_G$  has been investigated for slot rib waveguides by varying  $s$  in the range from 10 nm to 60 nm, for  $h=250$  nm,  $w=180$  nm and  $g=100$  nm. Also in this investigation, either vertical or non vertical ( $\theta = 8^\circ$ ) sidewalls have been considered, as sketched in Fig. 7. Both confinement factors decrease when  $s$  increases, as expected. Only when the cover medium is air,  $\Gamma_C$  remains practically constant with increasing  $s$ . Changing  $s$  from 0 (conventional slot waveguide) to 60 nm,  $\Gamma_C$  decreases about 30% and 10% for quasi-TE and quasi-TM mode, respectively.

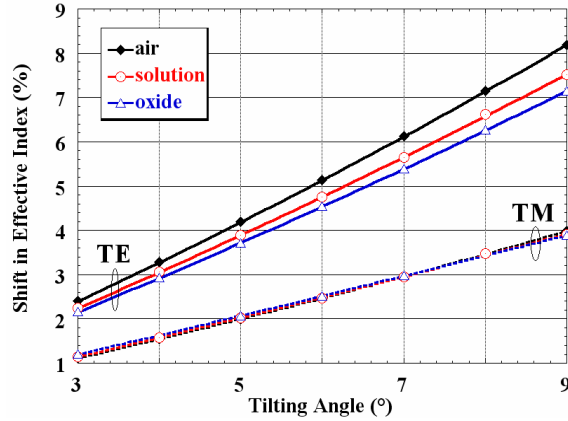


Fig. 6. Percentage shift of quasi-TE and quasi-TM mode effective indices (with respect to vertical case) as a function of non vertical sidewall tilting angle  $\theta$  ( $h=250$  nm,  $w=180$  nm,  $g=100$  nm,  $s=60$  nm), for a slot rib waveguide.

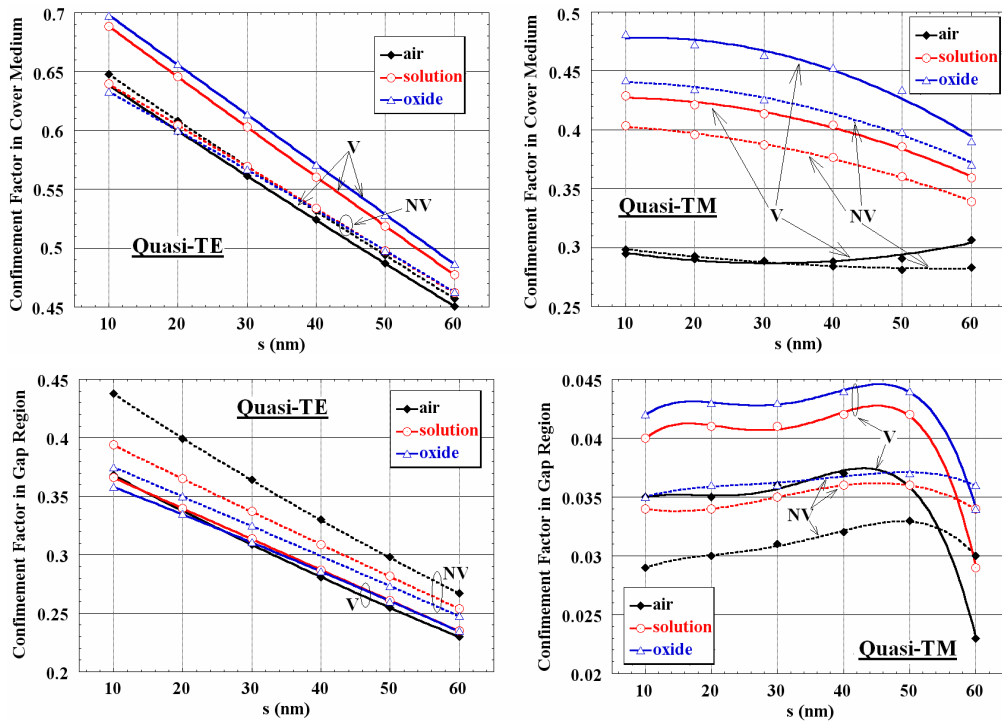


Fig. 7. SOI slot rib waveguide confinement factors in the cover medium and in the gap region dependence on  $s$ , assuming either vertical or non vertical ( $\theta = 8^\circ$ ) side-walls ( $h = 250$  nm,  $g = 100$  nm,  $w = 180$  nm).

### 3. Slot waveguide sensitivity

#### 3.1 Homogeneous sensing

Homogeneous sensing (effective index change of guiding structure due to cover medium refractive index change) enables to measure concentration of a wide spectrum of chemical species as glucose or ethanol, usually present in a solution. Moreover, this kind of sensing mechanism allows to estimate some gas concentration changes because some polymeric

materials have the refractive index sensitive to specific gas concentrations. In all these cases, a chemical analyte concentration change induces the refractive index change in a solid or a liquid material serving as cover medium in the guiding structure. For example, when glucose concentration in an aqueous solution changes, a shift of the solution refractive index is induced. In case of homogeneous sensing, waveguide sensitivity is defined as [20]:

$$S_h = \frac{\partial n_{eff}}{\partial n_c} \quad (2)$$

where  $n_{eff}$  is the propagating mode effective index. According with variational theorem for dielectric waveguides, we can write:

$$S_h = \left. \frac{\partial n_{eff}}{\partial n_c} \right|_{n_c=n_c^0} = \frac{2 n_c^0}{\eta_0 P} \iint_C |\mathbf{E}(x, y)|^2 dx dy = \frac{2 n_c^0 \Gamma_c}{\eta_0 P} \iint_{\infty} |\mathbf{E}(x, y)|^2 dx dy \quad (3)$$

where

$$P = \iint_{\infty} [(\mathbf{E} \times \mathbf{H}^* + \mathbf{E}^* \times \mathbf{H}) \cdot \hat{z}] dx dy \quad (4)$$

$\eta_0$  is the free space impedance,  $\mathbf{E}$  and  $\mathbf{H}$  are the electric and magnetic field vectors, respectively,  $\hat{z}$  indicates the unit vector along  $z$  direction (propagation direction) and  $n_c^0$  is the unperturbed value of cover medium refractive index. From Eq. (3), it is evident that waveguide sensitivity  $S_h$  proportionally depends on optical field confinement factor in the cover medium ( $\Gamma_c$ ). Because  $\Gamma_c$  monotonically decreases when  $s$  increases (being maximum for a conventional slot), the most appropriate guiding structure for homogeneous sensing is the conventional over the slot rib waveguide. That's why only sensitivity of conventional slot waveguides is presented in this sub-section. As defined by Eq. (2),  $S_h$  can be numerically estimated by varying the cover medium refractive index  $n_c$  in a narrow range and finding the relevant change of effective index  $n_{eff}$ . To determine effective index  $n_{eff}$ , the rigorous numerical approach based on 2D full-vectorial FEM has been applied.

An alternative perturbation approach for  $S_h$  estimation is that based on Eq. (3). In this case  $n_c$  value has to be maintained constant as equal to  $n_c^0$  value, and the two integrals in Eq (3) and (4) have to be calculated by FEM. The difference of sensitivity values calculated by using these two approaches is practically negligible (lower than 0.7%). Moreover, in mesh generation, the same parameters as in modal investigation have been used, giving very accurate results. In fact, an increase of number of mesh elements around 30% produces a change of estimated effective index lower than 0.004 % and a change of estimated  $S_h$  values lower than 0.05 %.

Conventional slot waveguide sensitivity  $S_h$  dependence on Si-wire width  $w$  has been investigated, for gap region width  $g$  equal to 100 nm and 200 nm and for quasi-TE and quasi-TM modes. The Si-wire height is assumed  $h=250$  nm. As cover medium, an aqueous solution containing a chemical substance (as, for example, glucose) whose concentration has to be measured, has been assumed. When analyte concentration in the solution changes, a shift in cover medium refractive index is induced. Its unperturbed value  $n_c^0$  has been fixed as 1.33, while cover medium refractive index changes in the range between 1.333 and 1.335. Either vertical or non vertical ( $\theta=8^\circ$ ) sidewalls have been considered (Fig. 8).

From data reported in Fig. 8, it is evident as quasi-TE mode is significantly more sensitive to cover medium refractive index change than quasi-TM one, in a conventional SOI slot waveguide. This difference is due to the large optical field confinement in the cover for quasi-TE with respect to quasi-TM mode. Either for quasi-TE or quasi-TM mode, conventional slot waveguide sensitivity monotonically decreases when  $w$  increases for  $g=100$  nm (considering either vertical or non vertical sidewalls) and for  $g=200$  nm (for non vertical sidewalls). For  $g=200$  nm and vertical sidewalls, sensitivity dependence on  $w$  exhibits a maximum of 0.932 for quasi-TE mode and 0.516 for quasi-TM mode (both corresponding to  $w=200$  nm). Assuming vertical sidewalls, the maximum sensitivity (0.959) is obtained for  $g=100$  nm,  $w=160$  nm and quasi-TE mode.



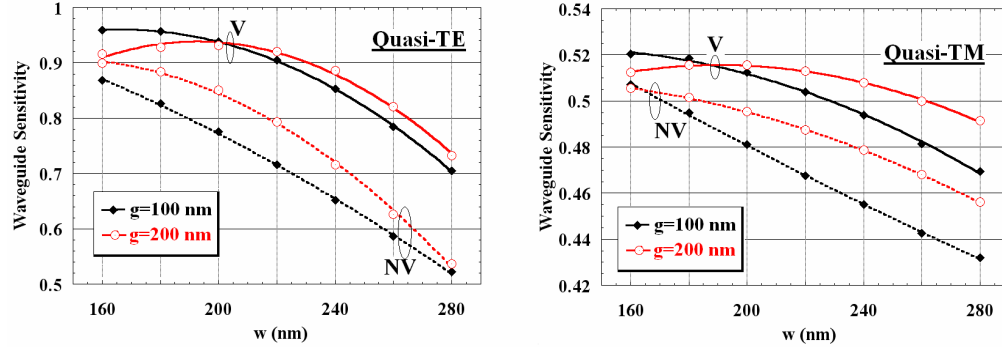


Fig. 8. Conventional SOI slot waveguide sensitivity dependence on  $w$ , for vertical and non vertical sidewalls ( $h=250$  nm).

Non vertical sidewalls significantly degrade the conventional slot waveguide sensitivity. This reduction is around 15% for quasi-TE (degradation increases until 25% when  $w$  increases) and around 5% for quasi-TM mode.

To maximize the sensitivity of conventional SOI slot waveguide, we have investigated the influence of  $h/w$  ratio. Assuming  $g=100$  nm, sensitivity has been calculated versus  $h/w$  ranging from 1.2 to 1.8, with  $w=140$  nm, 180 nm and 220 nm, respectively. Quasi-TE and quasi-TM modes have been again considered (see Fig. 9). For quasi-TE mode, sensitivity monotonically increases by increasing  $h/w$ , but the relevant slope decreases when  $w$  increases. For  $w=180$  nm and  $h/w=1.8$  (i.e.  $h=324$  nm), the maximum sensitivity has been obtained ( $S_h=1.0076$ ). For quasi-TM mode and  $w=140$  nm, sensitivity monotonically increases when  $h/w$  increases. For  $w=180$  nm, sensitivity dependence on  $h/w$  exhibits a maximum for  $h/w=1.4$ . Finally, for  $w=220$  nm, sensitivity monotonically decreases when  $h/w$  increases.

For  $w=180$  nm,  $h=324$  nm and for both polarizations, sensitivity dependence on  $g$  has been investigated (see Fig. 10). For quasi-TM mode,  $S_h$  quite linearly increases by increasing the gap region width whereas, for quasi-TE mode, the maximum sensitivity (1.0076) has been obtained exactly for  $g=100$  nm. This value is 70% larger than that obtained by a Si-wire waveguide proposed in literature [8] and it is more than one order of magnitude greater than that obtained by a rib waveguide [3]. Moreover, a value  $S_h > 1$  implies that an effective index change  $\Delta n_{eff} > \Delta n_c$  is induced by a cover index shift  $\Delta n_c$ .

A  $S_h$  value exceeding the unity is a quite counter-intuitive condition but the possibility that it verifies in some guiding structures characterized by a high confinement factor in the medium in which the refractive index changes, has been demonstrated and physically explained [21]. If a plane wave propagates in an homogeneous medium whose refractive index changes, its sensitivity is equal to 1. In an optical mode propagating in a guiding structure only a fraction of optical field propagates in the medium in which the refractive index changes, and then its sensitivity is expected to be lower than 1. This condition is quite usually verified in conventional guiding structures. It is necessary to underline that there are other important differences between the plane wave propagating in a medium having refractive index equal to  $n_c$  and the optical mode (quasi-TE or quasi-TM) propagating in a waveguide whose cover medium has the same refractive index  $n_c$ . The optical mode propagates more slowly because its effective index is larger than  $n_c$ . This difference of phase velocity  $v_p$  implies that, at a given power, the time-averaged density of energy in the medium having refractive index equal to  $n_c$  is larger when the optical mode propagates with respect to the case in which the plane wave propagates (i.e. time-averaged density of energy is proportional to  $1/v_p$ ).

Moreover, the electric field vector related to optical mode has non-zero components along all three axes (the electric field vector related to plane wave is in the transversal plane). These non-zero components contribute to  $S_h$ , because it can be expressed in the form:

$$S_h = \frac{2 n_c^0}{\eta_0 P} \left[ \iint_C |E_x|^2 dx dy + \iint_C |E_y|^2 dx dy + \iint_C |E_z|^2 dx dy \right] \quad (5)$$

where  $E_x$ ,  $E_y$  and  $E_z$  are the electric field vector component along  $x$ ,  $y$  and  $z$  axes, respectively (optical mode propagation is along  $z$ ).

Therefore, in a guiding structure in which confinement factor, in the medium whose refractive index changes, is large, the ratio  $n_{eff}/n_c$  is significantly larger than 1 and  $E_z$  is not negligible,  $S_h$  can exceed the unity.

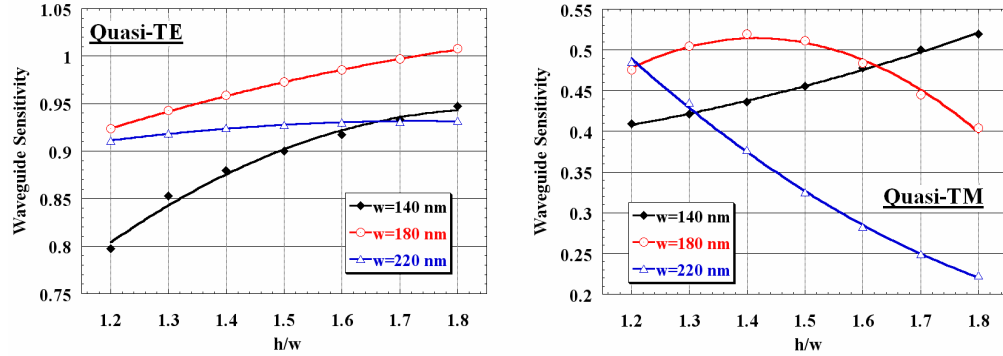


Fig. 9. Conventional SOI slot waveguide sensitivity versus  $h/w$ , for  $w=140$  nm, 180 nm and 220 nm ( $g=100$  nm).

Conventional slot waveguide sensitivity dependence on  $h/w$  can be analytically expressed by a quadratic polynomial. Thus we can write:

$$S_h = c_0 + c_1 \left( \frac{h}{w} \right) + c_2 \left( \frac{h}{w} \right)^2 \quad (6)$$

where  $c_0$ ,  $c_1$  and  $c_2$  are fitting parameters, whose values are reported in Table 1.

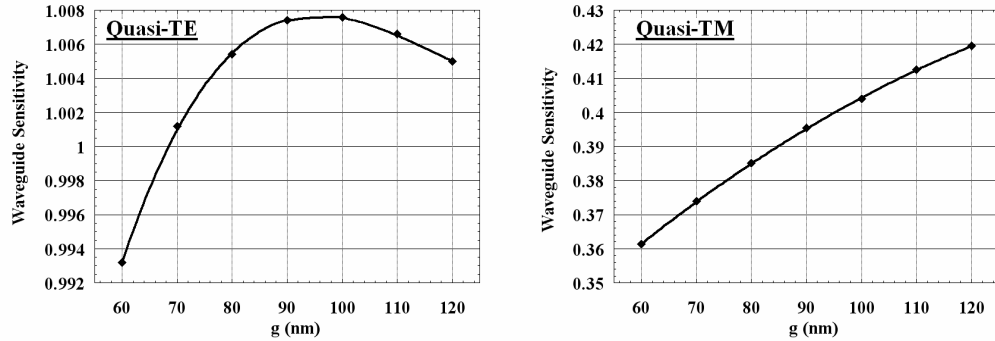


Fig. 10. Conventional SOI slot waveguide sensitivity as a function of  $g$  for quasi-TE and quasi-TM modes ( $w=180$  nm,  $h=324$  nm).

The conventional SOI slot waveguide, optimized for homogenous sensing with  $h=324$  nm,  $w=180$  nm and  $g=100$  nm, has been investigated for  $n_c=1.33$  (aqueous solution as cover medium) and assuming either vertical or non vertical ( $\theta=8^\circ$ ) sidewalls. Effective index, birefringence ( $B$ ) and confinement factor in the cover medium have been calculated, either for quasi-TE or quasi-TM modes, as it can be seen in Table 2.

Table 1. Fitting parameters of Eq. (6).

( $g=100$ nm)	$w$	$c_0$	$c_1$	$c_2$
Quasi-TE	140	-0.161	1.186	-0.318
	180	0.584	0.380	-0.080
	220	0.719	0.244	-0.070
Quasi-TM	140	0.390	-0.101	0.097
	180	-1.056	2.218	-0.783
	220	1.705	-1.390	0.314

Table 2. Parameters of conventional SOI slot waveguide optimized for homogeneous sensing.

Parameter ( $h=324$ nm, $g=100$ nm, $w=180$ nm)	Vertical	Non vertical
$n_{eff}$ (quasi-TE)	1.578638	2.050908
$n_{eff}$ (quasi-TM)	1.999899	2.209825
$B(n_{eff}^{TE} - n_{eff}^{TM})$	-0.421	-0.159
$\Gamma_C$ (quasi-TE)	0.7644	0.6549
$\Gamma_C$ (quasi-TM)	0.4117	0.3220
$S_h$ (quasi-TE)	1.0076	0.7146
$S_h$ (quasi-TM)	0.4040	0.2834

With the aim to compare the sensitivity of various SOI nanometer guiding structures, sensitivity dependence on waveguide width for either a SOI rib waveguide or a Si-wire waveguide (Fig. 11) has been investigated. In both cases we assume a waveguide height of 250 nm and an aqueous solution as cover medium (refractive index around 1.33). For SOI rib waveguide, an etch depth  $d_{RIB}=200$  nm has been fixed. Results are shown in Fig. 12, considering both quasi-TE and quasi-TM modes.

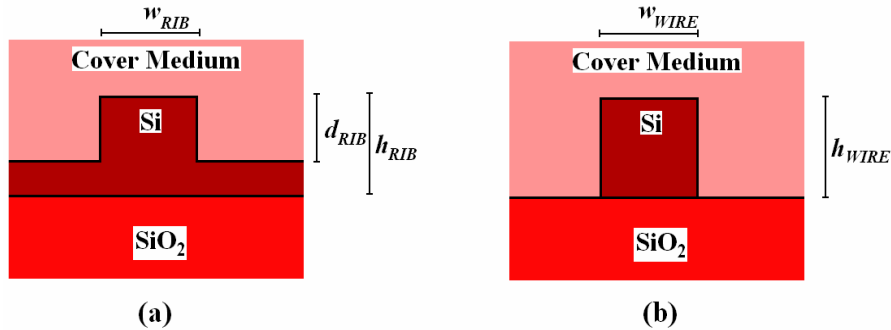


Fig. 11. (a) SOI rib waveguide structure. (b) Si-wire waveguide structure.

For SOI rib waveguide, quasi-TM assures a larger sensitivity than quasi-TE mode whereas, for a Si-wire waveguide, quasi-TM mode is more sensitive than quasi-TE one only for  $w_{WIRE} > 320$  nm. Moreover, it is possible to notice that Si-wire waveguide exhibits a higher sensitivity with respect to SOI rib waveguide in all considered cases, as expected. Maximum sensitivity obtainable by using Si-wire waveguide (relatively to considered set of parameters)

is 0.64 ( $h_{WIRE} = 260$  nm,  $w_{WIRE} = 300$  nm, quasi-TE mode). This value is two times larger than that experimentally obtained (0.31) for quasi-TM mode, using a Si-wire waveguide having  $h_{WIRE} = 260$  nm and  $w_{WIRE} = 450$  nm where quasi-TM mode is more sensitive than quasi-TE one [8]. It is also one order of magnitude larger than that experimentally obtained (0.061) for quasi-TM mode in a silicon nitride-on-oxide ( $\text{Si}_3\text{N}_4/\text{SiO}_2$ ) rib waveguide having  $h_{RIB} = 250$  nm,  $w_{RIB} = 4$   $\mu\text{m}$  and  $d_{RIB} = 4$  nm [3]. Moreover, the same value is 36% lower than that obtained by the conventional slot waveguide optimized for homogeneous sensing.

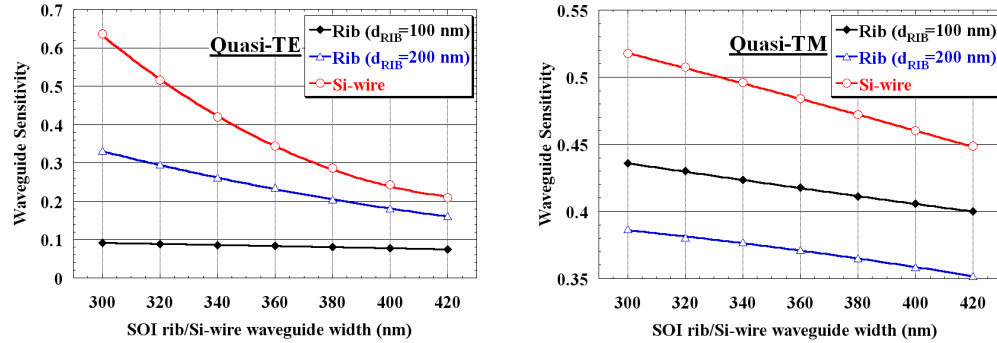


Fig. 12. SOI rib waveguide and Si-wire waveguide sensitivity as a function of waveguide width ( $h_{WIRE} = h_{RIB} = 250$  nm), quasi-TE and quasi-TM polarizations.

### 3.2 Surface sensing

Surface sensing is exploited in a wide range of biochemical applications, such as DNA sequencing by hybridization, antigen-antibody reactions study or pollution concentration measure in water. This kind of sensing is based on immobilization of an ultra-thin layer of receptor molecules on the guiding film surface. The interaction between analyte and receptor molecules produces a change of molecular adlayer thickness, affecting the effective index of propagating optical mode.

Conventional slot and slot rib waveguides can be used for surface sensing immobilizing an ultra-thin layer of receptor molecules on Si/cover medium interface (see Fig. 13).

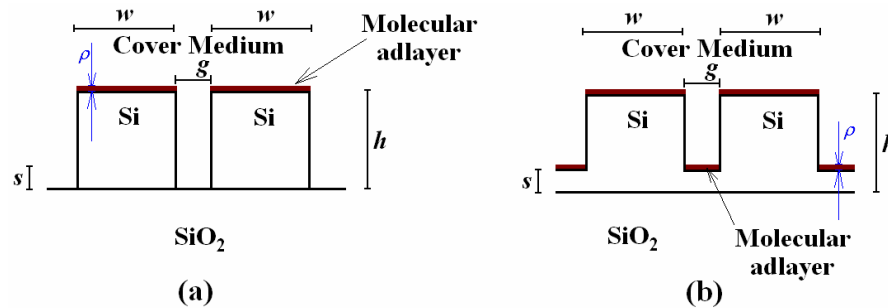


Fig. 13. SOI conventional slot (a) and slot rib (b) waveguides for surface sensing.

In case of surface sensing, waveguide sensitivity can be written as:

$$S_s = \frac{\partial n_{eff}}{\partial \rho} \quad (7)$$

where  $\rho$  is the molecular adlayer thickness. As defined in Eq. (7),  $S_s$  can be numerically estimated by varying  $\rho$  in a narrow range (from 2 nm to 4.8 nm, with step of 0.4nm) and determining the relevant change of effective index  $n_{eff}$ . To find the effective index  $n_{eff}$ , the rigorous numerical approach based on 2D full-vectorial FEM has been again applied, assuming the molecular adlayer refractive index as 1.45.

Shift of  $n_{eff}$  ( $\Delta n_{eff}$ ) due to a change  $\Delta\rho$  of adlayer thickness can be calculated by using a perturbation approach as:

$$\Delta n_{eff} = \frac{n_m^2 - (n_c^0)^2}{\eta_0 P} \iint_M |\mathbf{E}(x, y)|^2 dx dy \quad (8)$$

where  $n_m$  is the molecular adlayer refractive index and  $M$  is the region in which the adlayer thickness increases. Calculating  $S_s$  by this perturbation approach and by our numerical method based on Eq. (7), a difference lower than 4 % has been always observed.

In FEM mesh generation for  $S_s$  calculation, the same parameters as in modal investigation have been used. In molecular adlayer region, maximum element size is equal to 1 nm. The increase of number of mesh elements around 30 % produces a negligible change of surface sensitivity, lower than 0.4 %.

Assuming  $h=250$  nm, conventional slot waveguide surface sensitivity has been investigated as a function of Si-wire width  $w$ , for  $g$  equal to 100 nm and 200 nm and for both polarizations. As cover medium, an aqueous solution having a constant refractive index 1.33 has been again assumed. Molecular adlayer refractive index has been assumed as 1.45. Either vertical or non vertical ( $\theta=8^\circ$ ) sidewalls have been considered (Fig. 14).

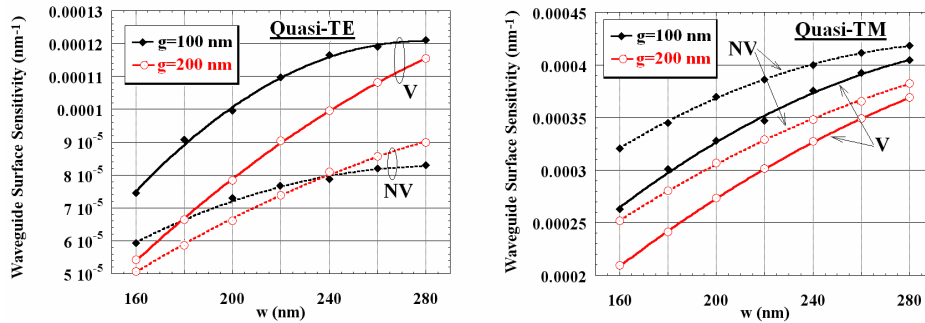


Fig. 14. SOI conventional slot waveguide surface sensitivity versus  $w$ , for vertical and non vertical sidewalls ( $h=250$  nm).

In conventional slot waveguide, quasi-TM mode is significantly more sensitive than quasi-TE one to deposited adlayer thickness increase. For both polarizations,  $S_s$  increases by increasing  $w$ . For quasi-TE mode, non vertical sidewalls produce a surface sensitivity decrease whereas, for quasi-TM mode, non verticality determinates a  $S_s$  increase. Maximum surface sensitivity ( $4.05 \times 10^{-4} \text{ nm}^{-1}$ ) is obtained for  $w=280$  nm,  $g=100$  nm and quasi-TM mode. For  $w=280$  nm,  $S_s$  dependence on gap region width has been investigated by considering both polarization (Fig. 15). For quasi-TM mode, surface sensitivity monotonically decreases when  $g$  increases whereas, for quasi-TE mode, surface sensitivity exhibits a maximum for  $g=70$  nm. For conventional slot waveguide, maximum  $S_s$  ( $4.31 \times 10^{-4} \text{ nm}^{-1}$ ) has been obtained when  $g=60$  nm,  $h=250$  nm,  $w=280$  nm (quasi-TM mode). This surface sensitivity value is more than two times larger than that ( $2 \times 10^{-4} \text{ nm}^{-1}$ ) obtainable by a  $\text{Si}_3\text{N}_4/\text{SiO}_2$  rib waveguide [22].

Slot rib waveguide sensitivity  $S_s$  dependence on silicon rib width  $w$  has been investigated, for a gap region width  $g$  equal to 100 nm and 200 nm, and for quasi-TE and quasi-TM mode. The waveguide total height is  $h=250$  nm and the silicon planar layer thickness is  $s=60$  nm (Fig. 16). For quasi-TE mode, surface sensitivity monotonically decreases by increasing  $w$ , with values obtained lower for  $g=100$  nm than for  $g=200$  nm. Surface sensitivity degradation produced by non vertical sidewalls is around 25% for  $g=100$  nm, and around 15% for  $g=200$  nm. For quasi-TM mode, surface sensitivity dependence on  $w$  exhibits a maximum for both considered values of  $g$  and when either vertical or non vertical sidewalls are assumed. Surface sensitivity degradation produced by non vertical sidewalls increases monotonically when  $w$  increases (this means a reduction around 15% for  $g=100$  nm and around 12% for  $g=200$  nm).

For  $g=100$  nm,  $w=220$  nm, quasi-TM mode and vertical sidewalls, the highest  $S_s$  value is obtained ( $3.98 \times 10^{-4}$  nm<sup>-1</sup>).

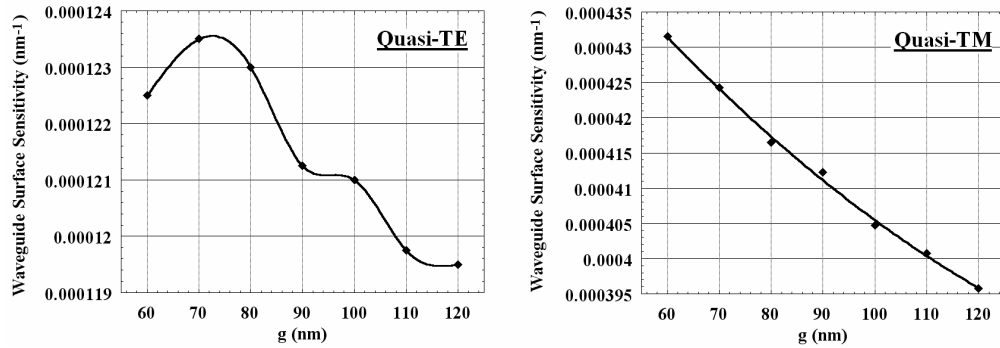


Fig. 15 Conventional slot waveguide surface sensitivity versus  $g$  ( $h=250$  nm,  $w=280$  nm), for vertical sidewalls.

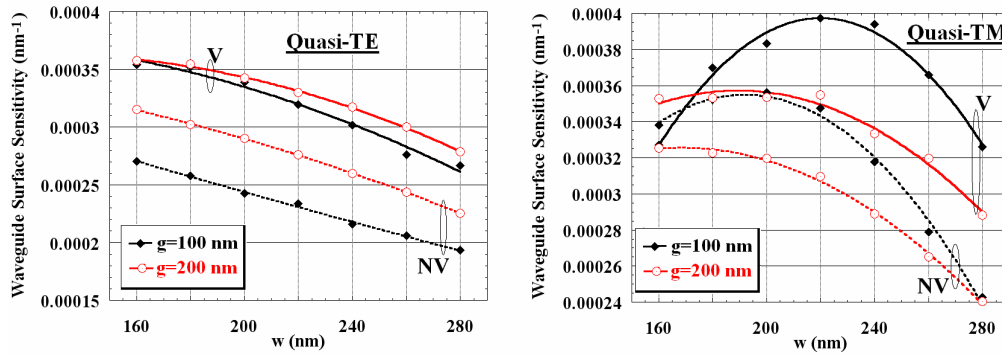


Fig. 16. SOI slot rib waveguide surface sensitivity dependence on  $w$ , for vertical and non vertical sidewalls ( $h=250$  nm,  $s=60$  nm).

Assuming  $w=220$  nm,  $g=100$  nm and  $h=250$  nm,  $S_s$  dependence on silicon planar layer thickness  $s$  has been also investigated, as shown in Fig. 17. SOI slot rib waveguide surface sensitivity monotonically decreases by increasing  $s$  and quasi-TM mode is more sensitive than quasi-TE one. To further optimize slot rib waveguide surface sensitivity,  $S_s$  dependence on  $g$  has been investigated with  $s=10$  nm,  $w=220$  nm and  $h=250$  nm (Fig. 18). For more sensitive case of quasi-TM mode,  $S_s$  decreases when  $g$  increases whereas for quasi-TE mode  $S_s$  increases when  $g$  increases. Maximum surface sensitivity ( $4.66 \times 10^{-4}$  nm<sup>-1</sup>) is obtained for  $g=60$  nm,  $s=10$  nm,  $w=220$  nm,  $h=250$  nm and quasi-TM mode. This value is 7% larger than that obtained using a conventional slot waveguide and it is more than two times greater than that obtainable by a Si<sub>3</sub>N<sub>4</sub>/SiO<sub>2</sub> rib waveguide [22].

The SOI slot rib waveguide optimized for surface sensing with  $g=60$  nm,  $s=10$  nm,  $w=220$  nm,  $h=250$  nm, has been investigated assuming either vertical or non vertical ( $\theta=8^\circ$ ) sidewalls. Effective index, birefringence ( $B$ ) and confinement factor in the cover medium have been calculated for both polarizations, and results are summarized in Table 3.

In case of surface sensing, a comparison between SOI slot (conventional and rib) and SOI rib and Si-wire (see Fig. 11 (a-b)) waveguides surface sensitivity has been also performed. For SOI rib waveguide, surface sensitivity dependence on ratio between etch depth  $d_{RIB}$  and waveguide total height  $h_{RIB}$  has been investigated. We assume a waveguide width  $w_{RIB}$  equal to 300 nm, an aqueous solution as cover medium (refractive index equal to 1.33) and deposited molecular layer refractive index equal to 1.45. Waveguide total height  $h_{RIB}$  has been assumed as 250 nm or 300 nm (Fig. 19).

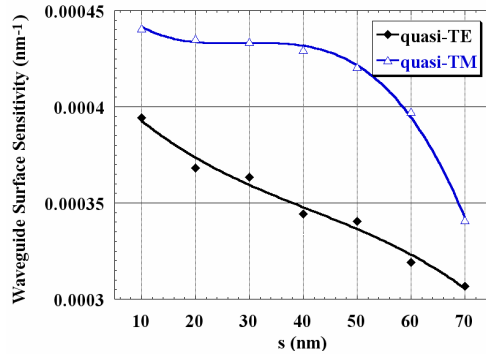


Fig. 17. SOI slot rib waveguide surface sensitivity as a function of  $s$  ( $h=250$  nm,  $g=100$  nm,  $w=220$  nm).

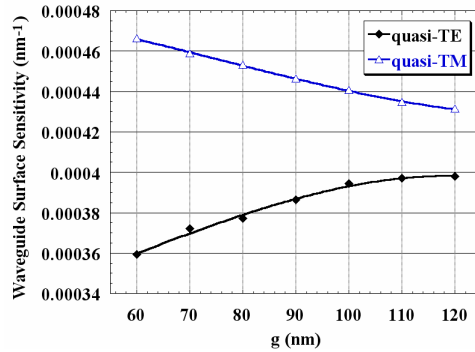


Fig. 18. SOI slot rib waveguide surface sensitivity as a function of  $g$  ( $h=250$  nm,  $s=10$  nm,  $w=220$  nm).

Table 3. Parameters of SOI slot rib waveguide optimized for surface sensing.

Parameter ( $h=250$ nm, $s=10$ nm, $w=220$ nm, $g=60$ nm)	Vertical	Non vertical
$n_{eff}$ (quasi-TE)	1.85062	2.254873
$n_{eff}$ (quasi-TM)	1.795375	1.901213
$B(n_{eff}^{TE} - n_{eff}^{TM})$	0.055	0.354
$\Gamma_C$ (quasi-TE)	0.663	0.498
$\Gamma_C$ (quasi-TM)	0.395	0.364
$S_h$ (quasi-TE)	$3.59 \times 10^{-4} \text{ nm}^{-1}$	$1.13 \times 10^{-4} \text{ nm}^{-1}$
$S_h$ (quasi-TM)	$4.66 \times 10^{-4} \text{ nm}^{-1}$	$4.48 \times 10^{-4} \text{ nm}^{-1}$

By increasing the  $d_{RIB}/h_{RIB}$  ratio, SOI rib waveguide surface sensitivity related to quasi-TE mode monotonically increases. For quasi-TM mode, surface sensitivity dependence on  $d_{RIB}/h_{RIB}$  ratio exhibits two points of local minimum ( $d_{RIB}/h_{RIB} = 0.5$  and  $0.7$ ) and a point of local maximum ( $d_{RIB}/h_{RIB} = 0.6$ ). Maximum surface sensitivity ( $5.05 \times 10^{-4} \text{ nm}^{-1}$ ) has been obtained for quasi-TM mode,  $h_{RIB} = 250$  nm and  $d_{RIB}/h_{RIB} = 0.2$  (i.e.  $d_{RIB} = 50$  nm). This value is quite similar to that obtained by the slot rib waveguide optimized for surface sensing (about



8% larger) and by the conventional slot guiding structure exhibiting maximum surface sensitivity (about 14% larger).

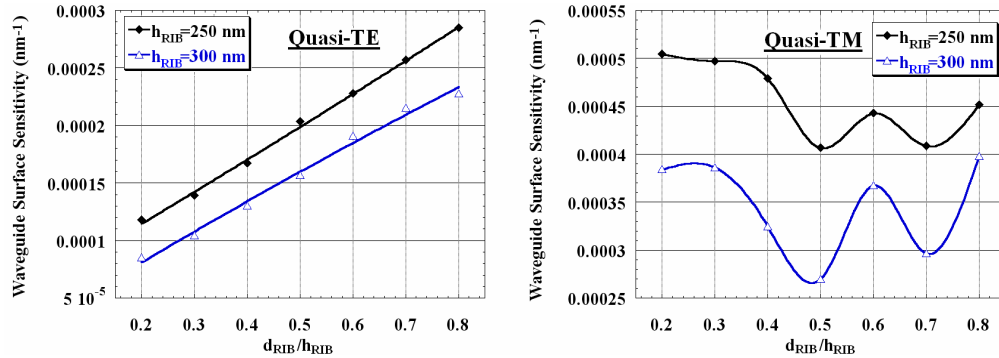


Fig. 19. SOI rib waveguide surface sensitivity dependence on  $d_{RIB}/h_{RIB}$  for quasi-TE and quasi-TM modes ( $w_{RIB} = 300$  nm).

For a Si wire waveguide, assuming a wire height  $h_{WIRE}$  of 250 nm or 300 nm, surface sensitivity dependence on wire width  $w_{WIRE}$  has been investigated (see Fig. 20). For quasi-TE mode (less sensitive than quasi-TM mode),  $S_s$  monolithically decreases when  $w_{WIRE}$  increases (for both considered values of  $h_{WIRE}$ ). For quasi-TM mode and wire height of 250 nm, surface sensitivity monotonically increases by increasing  $w_{WIRE}$  whereas, for the same polarization and  $h_{WIRE}=300$  nm,  $S_s$  decreases by increasing the wire width. Surface sensitivity maximum value obtained by a Si wire waveguide ( $4.76 \times 10^{-4}$  nm<sup>-1</sup>) is very similar to that exhibited by the slot rib waveguide optimized for surface sensing (about 2% larger).

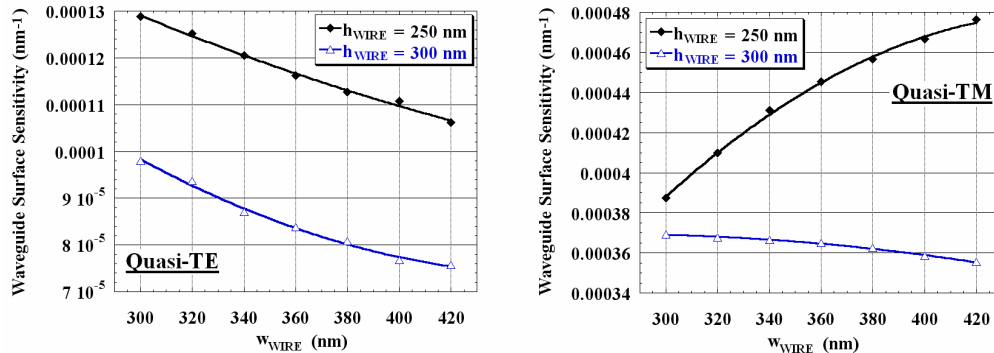


Fig. 20. Si-wire waveguide surface sensitivity versus  $w_{WIRE}$  for quasi-TE and quasi-TM modes ( $h_{WIRE} = 250$  and 300 nm).

#### 4. Conclusion

We have carried out a detailed investigation of modal properties and performance of silicon nanometer slot guiding structures. The employment of these waveguides for sensing purposes (chemical or biochemical) has been largely discussed.

Conventional slot waveguides have been proved to be very sensitive to cover medium refractive index change (homogeneous sensing), especially when a quasi-TE mode is considered. Using an optimized set of geometrical parameters, a sensitivity exceeding the unity can be obtained. This sensitivity value is significantly larger than those obtained by other nanometer guiding structures, although highly sensitive, such as Si-wires.

SOI slot rib waveguides constituted by two nanometer deeply etched SOI rib waveguides very close to each other have been also studied. The use of this guiding structure and of conventional slot waveguide for surface sensing has been discussed, demonstrating that



nanometer SOI rib, Si-wire and slot waveguides (conventional and rib) exhibit similar values of maximum surface sensitivity.

Non vertical sidewall influence on slot guiding structures has been investigated in terms of effective index, birefringence and sensitivity, with the result that conventional slot waveguides are more influenced than slot rib waveguides by this fabrication tolerance.

Because the sensitivity of integrated optical sensors strongly depends on their guiding structure, the results presented in this paper can be used as design criteria. Moreover, they are very encouraging for demonstrating that nanometer SOI slot waveguides can be exploited to fabricate ultra-sensitive and ultra-compact integrated optical chemical or biochemical sensors based on various architectures, such as Mach-Zehnder interferometer, directional coupler or microring resonator.

### **Acknowledgments**

This work has been partially supported by Italian Ministry for University and Research under Interlink Project n. II04C01CDM.